Original Article

MOLECULAR METABOLISM

Pancreatic, but not myeloid-cell, expression of interleukin-1alpha is required for maintenance of insulin secretion and whole body glucose homeostasis

J. Jason Collier [1,2], Heidi M. Batdorf [1], Thomas M. Martin [1,2], Kristen E. Rohli [1,6], David H. Burk [1], Danhong Lu [3], Chris R. Cooley [4], Michael D. Karlstad [4], Joseph W. Jackson [5,7], Tim E. Sparer [5], Jingying Zhang [1], Randall L. Mynatt [1], Susan J. Burke [1,*]

ABSTRACT

Objective: The expression of the interleukin-1 receptor type I (IL-1R) is enriched in pancreatic islet β-cells, signifying that ligands activating this pathway are important for the health and function of the insulin-secreting cell. Using isolated mouse, rat, and human islets, we identified the cytokine IL-1α as a highly inducible gene in response to IL-1R activation. In addition, IL-1α is elevated in mouse and rat models of obesity and Type 2 diabetes. Since less is known about the biology of IL-1α relative to IL-1β in pancreatic tissue, our objective was to investigate the contribution of IL-1α to pancreatic β-cell function and overall glucose homeostasis *in vivo*.

Methods: We generated a novel mouse line with conditional IL-1α alleles and subsequently produced mice with either pancreatic- or myeloid lineage-specific deletion of IL-1α.

Results: Using this *in vivo* approach, we discovered that pancreatic (IL-1α$^{Pdx1-/-}$), but not myeloid-cell, expression of IL-1α (IL-1α$^{LysM-/-}$) was required for the maintenance of whole body glucose homeostasis in both male and female mice. Moreover, pancreatic deletion of IL-1α led to impaired glucose tolerance with no change in insulin sensitivity. This observation was consistent with our finding that glucose-stimulated insulin secretion was reduced in islets isolated from IL-1α$^{Pdx1-/-}$ mice. Alternatively, IL-1α$^{LysM-/-}$ mice (male and female) did not have any detectable changes in glucose tolerance, respiratory quotient, physical activity, or food intake when compared with littermate controls.

Conclusions: Taken together, we conclude that there is an important physiological role for pancreatic IL-1α to promote glucose homeostasis by supporting glucose-stimulated insulin secretion and islet β-cell mass *in vivo*.

Keywords Cytokines; Cytokine receptors; Inflammation; Pancreatic islet; Rodent

1. INTRODUCTION

The cytokines interleukin-1 alpha (IL-1α) and interleukin-1 beta (IL-1β) were first discovered as signals that produce fever [1]; they are now known to be distinct proteins involved in a variety of cellular processes, including inflammation [2,3]. IL-1α and IL-1β both bind to the Type I interleukin-1 receptor (IL-1R) to alter biological activity [4]. Ligand-bound IL-1R connects these extracellular cytokine signals with intracellular activation of nuclear factor kappa B (NF-κB) and other key signaling pathways [5–7]. IL-1α is often produced in many cell types as part of the healthy tissue milieu [8,9], while IL-1β expression is primarily inducible in cells of the myeloid and lymphoid lineages [10,11]. In addition to regulatory control at the transcriptional level, each cytokine is synthesized in a precursor form and subsequently processed by distinct enzymatic complexes to achieve the mature form. In the case of IL-1α, calpain cleavage converts pro-IL-1α into mature IL-1α [12], while IL-1β is processed by the NLRP3 inflammasome complex [13].

Pancreatic β-cells in culture respond to both IL-1α and IL-1β through the aforementioned IL-1R [14–22]. However, IL-1β has been studied in much greater detail in islet biology compared with IL-1α. The outcome of exposing β-cells in culture to either IL-1α or IL-1β appears similar but varies by duration of stimulus. The acute outcome is to promote insulin release [14,22], while prolonged exposure (e.g., >6 h)

[1]Pennington Biomedical Research Center, Louisiana State University System, Baton Rouge, LA, 70808, USA [2]Department of Biological Sciences, Louisiana State University, Baton Rouge, LA, 70803, USA [3]Sarah W. Stedman Nutrition and Metabolism Center, Duke Molecular Physiology Institute, Duke University Medical Center, Durham, NC, 27704, USA [4]Department of Surgery, University of Tennessee Health Science Center, Knoxville, TN, 37920, USA [5]Department of Microbiology, University of Tennessee, Knoxville, TN, 37996, USA

[6] **Current Address**: Interdisciplinary Graduate Program in Genetics, Carver College of Medicine, University of Iowa, Iowa City, IA, 52242, USA.
[7] **Current Address**: Department of Microbiology and Molecular Genetics, University of Pittsburgh, School of Medicine, Pittsburgh, PA, 15219, USA.

*__Corresponding author__: Laboratory of Immunogenetics, Pennington Biomedical Research Center, Baton Rouge, LA, 70808, USA. E-mail: susan.burke@pbrc.edu (S.J. Burke).

Received June 25, 2020 • Revision received November 3, 2020 • Accepted December 2, 2020 • Available online 5 December 2020

https://doi.org/10.1016/j.molmet.2020.101140

leads to reductions in insulin secretion [16,23]. In addition, macrophage-derived IL-1β is also important for insulin secretion in response to physiological signals *in vivo* [24]. Likewise, pancreatic IL-1R is a major sensor controlling islet β-cell adaptive responses to aging and obesity *in vivo* [25]. Thus, physiological and pathophysiologic responses are both possible depending on the period of exposure and context of the IL-1R activating stimulus. However, to our knowledge, the tissue-specific role of IL-1α to impact endocrine pancreas function *in vivo* has not been investigated.

Therefore, we pursued in depth analyses of the biology of IL-1α using targeted deletion of this cytokine in cells of the myeloid lineage and from pancreatic tissue. Several key observations emerged from this approach: 1) IL-1α gene expression is robustly induced by IL-1β in mouse, rat, and human islets as well as rat β-cell lines. 2) IL-1α expression is greater in Zucker Diabetic Fatty (ZDF) rats and *db/db* mice, commonly used rodent models of obesity and Type 2 diabetes, than in lean controls. 3) Tissue-specific loss of function approaches reveal that pancreatic IL-1α is required to maintain glucose homeostasis *in vivo*, while deletion of IL-1α from cells of the myeloid lineage does not contribute to glucose tolerance, energy expenditure, or physical activity. Taken together, our results reveal a physiological role for pancreatic IL-1α to support healthy islet function and whole body glucose homeostasis.

2. MATERIALS AND METHODS

2.1. Cell culture, islet isolation, and reagents

IL-1β was purchased from Peprotech (Rocky Hill, NJ). Lipopolysaccharides (LPS) were from InvivoGen (San Diego, CA). Culture of the 832/13 and INS-1E rat insulinoma cell lines has been described previously [26]. Raw 264.7 cells were from ATCC (Manassas, VA). All cell lines were confirmed to be free of mycoplasma contamination. Seven-week-old male *db/+* and *db/db* mice (B6.BKS(D)-Lepr^{db}/J mice; Stock # 000697) were purchased from the Jackson Laboratory (Bar Harbor, ME). Mice with a targeted deletion of IL-1R in pancreatic tissue (IL-1R$^{Pdx1-/-}$) were described previously (25). Islets were isolated from female IL-1R$^{Pdx1-/-}$ and littermate control mice (IL-1R$^{fl/fl}$) between 8 and 10 months of age. Our procedure for isolation of mouse islets was described in detail [27]. Human islets were obtained from Lonza (Clonetics™) on 3 separate occasions. Each shipment was from a separate donor and subsequently handpicked into duplicates for each biological replicate used for cytokine treatment. The known donor data are reported in Supplementary Table 1. Seven-week-old male Wistar (Strain #003), *fa/+* and *fa/fa* rats (ZDF-Lepr^{fa}/Crl; Stock #370 and 380, respectively) were purchased from Charles River (Wilmington, MA). All animals were allowed to acclimate for a minimum of 1 week with *ad libitum* access to food and water prior to isolation of pancreatic islets. Our procedure for rat islet isolation is as follows: an enzyme collagenase solution (13 mL) was prepared per rat containing 1X HBSS, 4 mM of sodium bicarbonate (7.5% solution added at 4.7 mL/L), 250 μL of cold 1M HEPES buffer (Gibco, Grand Island, NY), 12 μL of DNase 1 (100 mg/mL) (Roche, Indianapolis, IN), and 1 mL Liberase TL (2.5 mg/mL) (Roche). The enzyme solution (4 mL) for each rat was drawn up into a 5-mL syringe and kept on ice. Rats were euthanized via CO_2 asphyxiation followed by a cervical dislocation. The fur was wetted with 70% ethanol, and a V-shaped incision was made to expose the peritoneal cavity. The pancreas was perfused after cannulation of the common bile duct with a 27-g blunt needle held in place with a ligature and the ampulla of Vater clamped with hemostats, followed by slow infusion of the enzyme solution. After perfusion, the pancreas was excised and placed in a 50-mL Falcon tube containing roughly 9 mL of the enzyme solution. The pancreas was periodically shaken while incubating for 30 min in a 37 °C water bath. After 30 min, the pancreas was shaken vigorously for 10 s before digestion was stopped with 40 mL of quenching buffer (1X HBSS, 4 mM of sodium bicarbonate, 27.5 mL of fetal bovine serum (FBS), and 50 μL of DNase at 100 mg/mL). This mixture was plunged several times through a 14-g blunt-tipped needle to further homogenize the tissue. The homogenate was passed through a 400-μm screen (Bellco, Vineland, NJ) into a new Falcon tube to filter out large pieces of undigested exocrine tissue. The tube was centrifuged at 252 *g* at 4 °C for 3 min, after which the supernatant was discarded. The pellet was suspended in a separate Falcon tube with 7 mL of a Polysucrose 400 (MP Biomedical, Pittsburgh, PA) solution at 1.109 g/mL. A gradient was then produced by carefully layering 7 mL of 1.096 g/mL on top, followed by 1.070 g/mL and 0.570 g/mL. This solution was centrifuged at 920 *g* for 20 min at 4 °C. The islets were located at the interface between the 1.070 g/mL and 0.570 g/mL layers, and a bulb pipette was used to extract the islets from the layer and into a new tube containing 40 mL of quenching buffer. The islets were washed in quenching buffer by centrifuging at 250 g for 3 min. The supernatant was discarded, and the wash step was repeated. The resulting pellet was suspended in 10 mL of 1640 RPMI media supplemented with 10% fetal bovine serum (FBS), penicillin (10,000 units/mL), streptomycin (10,000 μg/mL), amphotericin B (250 mg/mL), and glucose (11 mM) and subsequently plated. Islets were imaged using an Olympus CK40 inverted microscope for hand-picking. Islets were incubated at 37 °C and 5% CO_2 for 24 h and further handpicked into a clean plate after incubation for downstream applications.

2.1.1. Generation of mice with conditional interleukin 1-alpha alleles

The knock-out first (aka 'targeted trap'), reporter-tagged targeting vector was purchased from EUCOMM (ID# 371319), consisting of 4.5 kb of 5'arm and 3.6 kb of 3'arm for homologous recombination. For gene targeting, 50 μg of linearized targeting vector was electroporated into B6 ES cells. Correct homologous recombination in targeted clones was confirmed by Fidelity PCR (polymerase chain reaction) at the 5′-end and 3′-end. The fragments produced from Fidelity PCR with these primers were sequenced to further verify the correctness of recombination. Three different colonies of targeted ES cells were injected into Albino-B6 blastocysts, and germline transmitting chimeric mice were obtained and then mated with Albino-B6 mice to generate heterozygous offspring on a B6 background. The mice used in this study were all on a mixed B6J; B6N genetic background.

2.1.2. Generation and use of mice with pancreas and myeloid-targeted deletion of IL-1α

Mice with pancreas- and myeloid-specific deletions of IL-1α were generated by crossing IL-1α floxed mice with Pdx1-cre (Stock # 014647; The Jackson Laboratory, Bar Harbor, Maine) or LysM-cre mice (Stock #004781), respectively. Mice were group-housed with a 12-hour light/12-hour dark cycle in a temperature- (22 ± 2 °C) controlled room with *ad libitum* access to Rodent Diet 5015 (LabDiet, St. Louis, MO) and water. At least four separate cohorts of mice were bred to complete this study (both Pdx1-cre and LysM-cre), and both male and female mice were used. In addition, only one copy of the cre allele (hemizygous) was used to generate mice with gene deletions. The number of animals for each individual experiment is stated in the relevant figure legend. Measurements of body composition were assessed by NMR using a Bruker Minispec LF110 Time-Domain NMR

system. For measurements of energy expenditure, respiratory quotient, activity, sleep, and caloric intake, a separate cohort of 3-month-old mice were monitored using metabolic cages (TSE Systems or Sable Systems Promethion). Briefly, these animals were single-housed and allowed to acclimate to training cages for 1 week before the start of metabolic measurements [28]. Upon completion of each study group, animals were fasted for 4 h, followed by CO_2 asphyxiation, and euthanization by decapitation. Trunk blood was collected for serum fraction extraction. Liver and fat depots were snap frozen in liquid nitrogen, and pancreata were fixed in 10% neutral-buffered formalin. All animal procedures described herein were approved by the respective Pennington Biomedical Research Center, Duke University, or University of Tennessee Medical Center Institutional Care and Use Committees.

2.1.3. Glucose and insulin tolerance tests (GTT and ITT), *ex vivo* GSIS, indirect calorimetry, and serum insulin measurements

ITT and GTTs were performed in male and female IL-1$\alpha^{Pdx1-/-}$ and IL-1$\alpha^{LysM-/-}$ mice following a 2- and 4-h fast, respectively. Procedures were performed as described previously [28,29]. Briefly, Humulin R insulin (Lilly, Indianapolis, IN) was administered at 0.75 U/kg body weight via intraperitoneal (i.p.) injection following a 2-h fast. Blood samples were taken from the tail vein immediately before the injection, as well as at the times indicated after injection. Blood glucose was measured with an ACCU-CHEK Aviva PLUS Glucometer (Roche Diagnostics, Indianapolis, IN). Blood glucose levels were plotted against time, and the area under the curve was calculated. GTTs were conducted after a 4-h fast by i.p. injection of 2.5 g of glucose/kg body weight. Perifusion analyses of insulin secretion using isolated islets of similar size from 4-month-old male IL-1$\alpha^{fl/fl}$ and IL-1$\alpha^{Pdx1-/-}$ mice were performed by the Islet Procurement and Analysis Core at Vanderbilt University as previously described [25,30]. For measurements of energy expenditure (EE), activity, and sleep time, mice were acclimated to the training cages for 1 week. In the metabolic cage, corn cob bedding was included, and there was an intake manifold (a small metal tube that runs along the perimeter of the cage to pull air). The training cage was exactly the same (bedding, dimensions, etc.) as the testing cage, minus the manifold on the perimeter of the cage. Mice were single-housed in the training cages and also in the metabolic cages during measurements. All animals were allowed free access to water and food during metabolic cage measurements. Serum insulin was measured using the Mouse Insulin ELISA kit from Mercodia (Uppsala, Sweden) according to the manufacturer's instruction.

2.1.4. RNA extraction, cDNA synthesis, real-time reverse transcription PCR (RT-PCR), and immunoblotting

832/13, INS-1E, and Raw 264.7 cells were cultured and treated in 12-well plates. Total RNA was extracted from cell lines using TRI Reagent (Sigma, St Louis, MO). Total RNA was extracted from isolated islets and eWAT tissue using the RNeasy Mini RNA kit (Qiagen) and from liver tissue using the Quick-RNA Miniprep kit (Zymo Research, Irvine, CA). Our methods and reagents for cDNA synthesis, primer design, and transcript analysis have been described in detail previously [31]. Transcript levels were normalized to the housekeeping gene Rs9. For detection of proteins by immunochemical analyses, islets isolated from IL-1$\alpha^{fl/fl}$ and IL-1$\alpha^{Pdx1-/-}$ mice (300 islets per genotype were pooled from 3 mice). The islets were treated with 10 ng/mL of IL-1β for 4 h and then lysed in 300 μL M-PER lysis reagent (Thermo Fisher Scientific) supplemented with Halt Protease and Phosphatase Inhibitor Cocktail (Thermo Fisher Scientific). Protein was quantified using a BCA assay. Denaturation of samples and immunoblotting conditions have been described [29]. Densitometry was performed using Image Lab software (Bio-Rad) to calculate the % change between genotypes. Antibodies were from Abcam (IL-1α Cat # ab7632) and Cell Signaling technology (β-Actin Cat # 8457).

2.1.5. Bone marrow-derived macrophages, peritoneal exudate cell (PECs) isolation, flow cytometry, and IL-1α enzyme-linked immunosorbent assay (ELISA)

Mice were intraperitoneally injected with 3% Brewer's thioglycollate. Four days after injection, all mice were euthanized, and peritoneal exudate was harvested. Ammonium-chloride-potassium (ACK) lysis buffer was used to remove erythrocytes from extracted peritoneal exudate. Live cells were identified using the ThermoFisher Near IR LIVE/DEAD stain. We used this live single-cell population in subsequent analyses. For flow cytometry, single-cell suspensions of PECs were stained with fluorochrome-conjugated antibodies against CD11b (M1/70), F4/80 (BM8), or Ly6G (1A8), CD3 (17A2), B220 (RA3-6b2) (Biolegend). Single cells were gated based on SSC-W/SSC-A and FSC-W/FSC-A and used for subsequent analysis. Data were acquired on a BD LSR II flow cytometer (BD Biosciences) and analyzed using FlowJo Software, version 10.1. Peritoneal exudate cells (PECs) were plated onto non-tissue culture-treated plates for 3 h to allow the adherence of macrophages. After washing off non-adherent cells, PEC macrophages were exposed to LPS at a concentration of 10 μg/mL for 3 h. The culture medium was removed and cells resuspended in RLT (Qiagen) for downstream RNA extraction and analysis, combining 3 wells for approximately 3×10^6 macrophages per replicate. Additionally, bone marrow was harvested from the femurs of 3 mice per strain. Bone marrow-derived macrophages (BMDMs) were differentiated in 10 ng/mL of M-CSF (Peprotech) with media replaced every 3 days. At day 9, macrophages were stimulated with LPS from *E. coli* 0111:B4 (LPS-EB; Invivogen) at 10 μg/mL for 3 h and resuspended in either RLT for downstream RNA extraction and analysis, or radioimmunoprecipitation assay (RIPA) buffer with protease inhibitors for protein analysis, i.e., ELISA confirmation of genetic reduction using a mouse IL-1α Quantikine ELISA kit from R&D Systems, Inc. (Cat # MLA00).

2.1.6. Pancreas histology and immunohistochemistry

After fixation in 10% neutral buffered formalin (NBF) for 24–48 h, the pancreatic tissue was embedded in paraffin. Five-microgram sections were cut onto positively charged slides for immunohistochemical (IHC) analyses. Detection of insulin was performed on a Leica Bond-Max (Leica Biosystems, Melbourne, Australia) using the Bond Polymer Refine detection kit. Primary antibodies used were guinea pig anti-insulin (1:800, #18–0067, Invitrogen, Grand Island, NY) and cre recombinanse (CST# 15036) followed by 30 min with horseradish peroxidase (HRP)-conjugated rabbit anti-guinea pig (1:800, A5545, Sigma, Saint Louis, MO). Stained sections were imaged using a Hamamatsu NanoZoomer digital slide scanner at 20x resolution. For determination of insulin-positive area, insulin-positive islets were detected using insulin staining from FFPE pancreatic tissue. Multiple sections were typically cut from each mouse for downstream IHC applications. These sections were analyzed and quantified using a custom application that detects insulin positive area for each islet present within a section using the Visiopharm VIS software version 5.0.5. The total number of islets counted was 1,600–2,000 across knockouts and littermate controls. For measurements of beta-cell

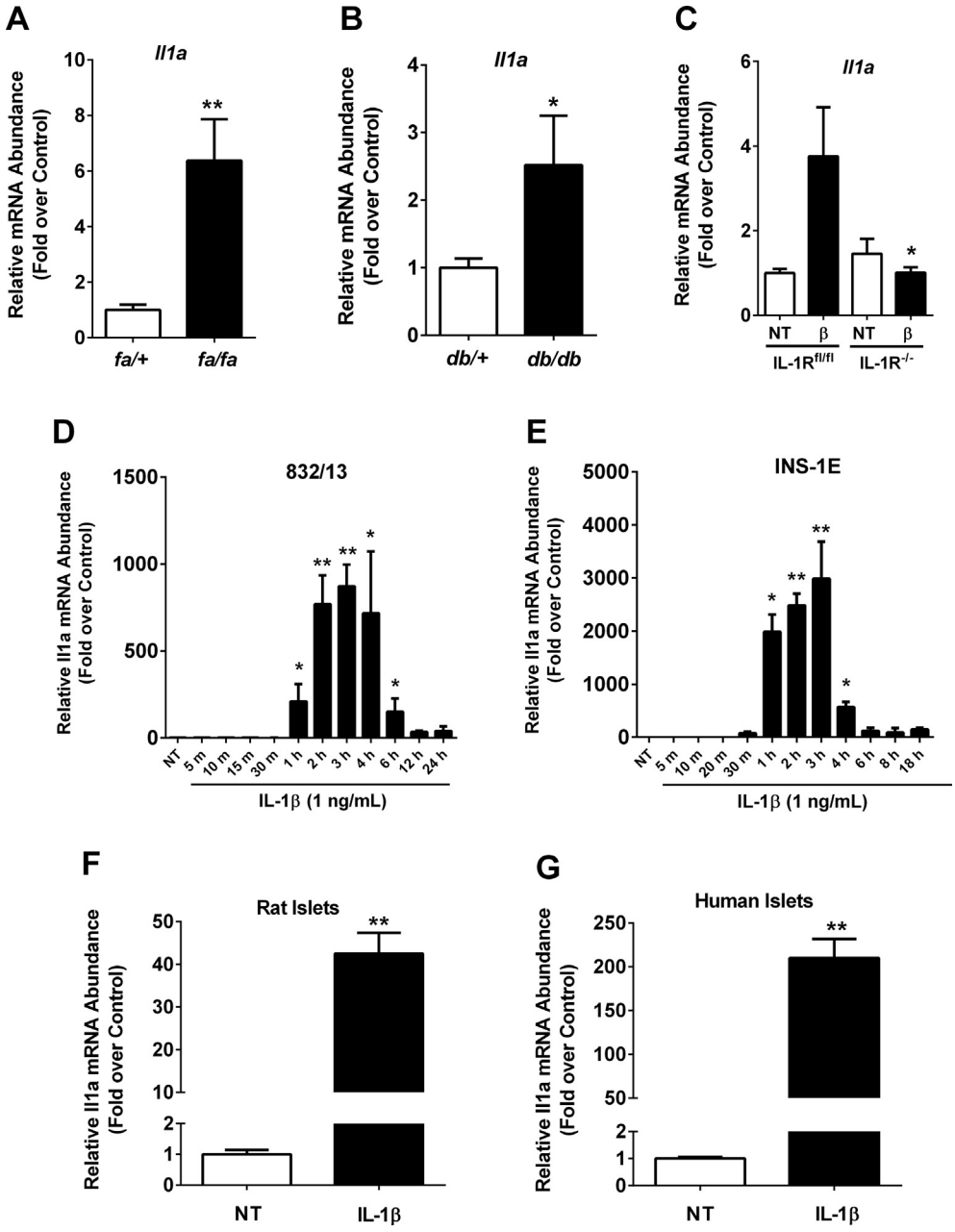

Figure 1: Expression of the *Il1a* gene is enhanced in response to IL-1β in lean mice and increased in the islets of obese rodents. (A) Islets isolated from 8-week-old male *fa/+* and *fa/fa* rats, and (B) male (8 week old) *db/+* and *db/db* mice. (C) Islets isolated from female IL-1R$^{fl/fl}$ and IL-1R$^{Pdx1-/-}$ mice were untreated (NT) or treated with 10 ng/mL IL-1β for 3 h. (D) 832/13 rat insulinoma cells and (E) INS-1E insulinoma cells were either untreated (NT) or treated with 1 ng/mL of IL-1β for the indicated times. (F) Isolated rat and (G) human islets were either untreated or stimulated with 10 ng/mL IL-1β for 3 h. (A–G) *Il1a* transcript data are shown as means ± SEM from 3 to 6 individual experiments. **, $p < 0.01$ vs. NT; *, $p < 0.05$ vs. NT.

mass, the ratio of insulin positive area to pancreatic area was multiplied by the pancreas wet weight. Measurements of the major and minor axis were conducted using a custom Visiopharm application that was developed to fit an ellipse to each identified islet and report the measured axis lengths.

2.1.7. Statistical analysis

Statistical analysis was performed using GraphPad Prism 6.07 (GraphPad Software, La Jolla, CA). Data were analyzed by two-tailed Student's t-test, one-way analysis of variance (ANOVA) using a Tukey's post hoc, or repeated-measures ANOVA (for longitudinal measures of body weight and body composition). Data are represented as means ± SEM.

3. RESULTS

3.1. Il1a gene expression is increased in pancreatic islets from obese rodents and in response to pro-inflammatory signals

The presence of IL-1β within islets of obese rats and mice has been established [16,25,32]. In addition, the requirement for IL-1R to

support insulin secretion and islet β-cell mass expansion *in vivo* highlighted the importance of this pathway during obesity and aging [25]. Thus, we screened islets isolated from well-established rat and mouse models of obesity for the expression of IL-1α, the other ligand responsible for activating IL-1R. Using islets isolated from 8-week-old male ZDF rats (*fa/fa*) and male *db/db* mice, we determined that expression of the *Il1a* gene is elevated 7.3, and 2.6-fold, respectively, when compared to age-matched heterozygous lean controls (*fa/+*; Figure 1A and *db/+*; Figure 1B). Next, we established that expression of the *Il1a* gene is induced 3.8-fold upon exposure of islets from female IL-1R$^{fl/fl}$ mice to the pro-inflammatory cytokine IL-1β. This response is completely abrogated in mice with a pancreas-specific deletion of the IL-1R (Figure 1C). Because of the ability of IL-1β to enhance the expression of IL-1α, we conducted a time course analysis using rat insulinoma cells, which revealed that the *Il1a* gene was induced within one hour after exposure to IL-1β, reaching maximal expression levels between 2 and 4 h, and gradually diminishing back to baseline by 12 h post-treatment (832/13 cells; Figure 1D). Similar results were obtained using the rat INS-1E β-cell line (Figure 1E). Furthermore, expression of the *Il1a* gene was induced 42.9- and 234.7-fold in response to IL-1β in islets isolated from rats (Figure 1F) and humans (Figure 1G), respectively. Taken together, *Il1a* expression was enriched in islets from obese mice and rats as well as inducible in culture models in response to IL-1β.

3.2. Deletion of IL-1α in pancreatic tissue impaired whole body glucose tolerance in male mice

Given the striking increase in *Il1a* gene expression in isolated islets of obese animals (Figure 1A,B), as well as in response to pro-inflammatory stimuli (Figure 1C–G), we tested the hypothesis that IL-1α within pancreatic tissue regulates islet β-cell function and mass. This required the generation of a mouse with conditional alleles (IL-1α$^{fl/fl}$), which we then crossed with mice expressing *cre* recombinase under the control of the Pdx1 promoter to generate a pancreas targeted deletion (IL-1α$^{Pdx1-/-}$). Expression of the *Il1a* gene is consequently decreased by 79.5% in islets isolated from IL-1α$^{Pdx1-/-}$ mice relative to controls (Figure 2A); the cycle threshold values for *cre* expression averaged 39.7 in mice that genotyped homozygous floxed and cre-negative versus a value of 26.6 in mice homozygous for the floxed allele and hemizygous for cre (Figure 2B). This is consistent with staining for cre protein in the nucleus of pancreatic islet cells (Supplementary Fig. 1A). Reduced expression of the *Il1a* gene in IL-1α$^{Pdx1-/-}$ mice was effectively targeted to islets and no significant decrease in gene expression was observed in either liver or the epididymal white adipose tissue (eWAT; data not shown). Basal levels of IL-1α protein were barely detectable in islets isolated from IL-1α$^{fl/fl}$ and IL-1α$^{Pdx1-/-}$ mice (not shown). However, upon treatment with the pro-inflammatory cytokine IL-1β, abundance of the IL-1α protein was readily detectable in control mice and decreased by 51% in islets isolated from IL-1α$^{Pdx1-/-}$ mice relative to control mice (Figure 2C). Residual IL-1α protein detected in IL-1α$^{Pdx1-/-}$ mice via immunoblot is likely due to the presence of cells that do not express Pdx-1 (e.g., macrophages, fibroblasts, etc.).

Total body mass was not different between groups as male mice aged (Figure 2D). In addition, body mass and blood glucose levels were similar between non-floxed cre-negative and non-floxed cre-positive mice (Supplementary Figs. 1B and 1C). Furthermore, no observable differences were present in whole-body fat (Figure 2E) or fluid (Figure 2G) mass in IL-1α$^{Pdx1-/-}$ animals relative to control mice; however, a decrease in lean mass was observed in older IL-1α$^{Pdx1-/-}$ mice beginning at 8 months of age (Figure 2F). There was no significant change in insulin sensitivity in 2-month-old male mice (Figure 2J) between IL-1α$^{Pdx1-/-}$ mice and littermate controls. In addition, glucose tolerance (Supplementary Figs. 1D and 1E), serum insulin (Supplementary Fig. 1F), and insulin positive area (Supplementary Fig. 1G) are similar between non-floxed cre-negative and non-floxed cre-positive mice. Deletion of IL-1α in pancreatic tissue does not impact whole body glucose homeostasis in 4-month-old male mice (Figure 2H,I); however, by 8 months of age, fasting glucose levels are significantly elevated in IL-1α$^{Pdx1-/-}$ mice compared to controls, and glucose intolerance is evident in the older cohort (Figure 2K,L).

3.3. Deletion of IL-1α in pancreatic tissue reduced whole body glucose tolerance in female mice

In female mice, body composition changes occur between groups in an age-related manner with significant elevations in body mass (Figure 3A), fat mass (Figure 3B), lean mass (Figure 3C), and fluid mass (Figure 3D) occurring in IL-1α$^{Pdx1-/-}$ mice compared to control mice between 5 and 8 months of age. Although insulin sensitivity is unchanged between groups (Figure 3E), there is a modest glucose intolerance in IL-1α$^{Pdx1-/-}$ mice by 4 months of age (Figure 3F,G) that is exacerbated at 8 months of age (Figure 3H,I). Although no insulin resistance is detected using an ITT, serum insulin concentrations are significantly higher in 9 month old IL-1α$^{Pdx1-/-}$ female mice (Figure 3J). Insulin positive area is reduced compared to controls (Figure 3K), although there is no significant difference in islet fraction between the genotypes (Figure 3L). Furthermore, no difference was seen in the major or minor axis length of islets between genotypes in female mice (data not shown).

3.4. Pancreatic deletion of IL-1α does not modify EE, RER, activity, or caloric intake

Using a separate cohort of male mice, we assessed whether the glucose intolerance evident in IL-1α$^{Pdx1-/-}$ mice compared to littermate controls could explain differences in energy expenditure (EE), food intake, or other metabolic parameters. We found that neither daily nor mean EE assessed over a 6-d period was different between groups (Figure 4A,B). Similarly, there were no discernible changes in respiratory exchange quotient (Figure 4C,D) or activity levels cumulatively or when broken down by light and dark intervals (Figure 4E,F). Furthermore, both IL-1α$^{fl/fl}$ and IL-1α$^{Pdx1-/-}$ mice consumed similar amounts of solid food (Figure 4G) and drank water in near identical quantities (Figure 4H).

3.5. IL-1α$^{Pdx1-/-}$ mice have a reduction in both glucose-stimulated insulin secretion and β-cell mass

Because insulin tolerance was similar between IL-1α$^{fl/fl}$ and IL-1α$^{Pdx1-/-}$ mice (Figure 2J), but glucose tolerance was impaired (Figure 2K,L), we next investigated insulin secretion in response to glucose or KCl. Perifusion analyses using islets isolated from male mice revealed a decrease in glucose-stimulated, but not KCl-induced, insulin release in islets isolated from IL-1α$^{Pdx1-/-}$ mice (Figure 5A). Quantification of maximal glucose-stimulated insulin secretion revealed 25.8% less output in IL-1α$^{Pdx1-/-}$ mice compared to littermate controls (Figure 5B). These findings were not explained by a loss in islet insulin content in IL-1α$^{Pdx1-/-}$ mice (Figure 5C). In a separate cohort of mice, static incubation assays also confirm that insulin content is similar between genotypes (Supplementary Fig. 2A), while there is a clear reduction in glucose-stimulated insulin secretion *ex vivo* (Supplementary Fig. 2B). The expression of the *Ins1* and *Ins2* genes were not different between genotypes (Supplementary Figs. 2C and 2D). Although insulin secretion in response to glucose was

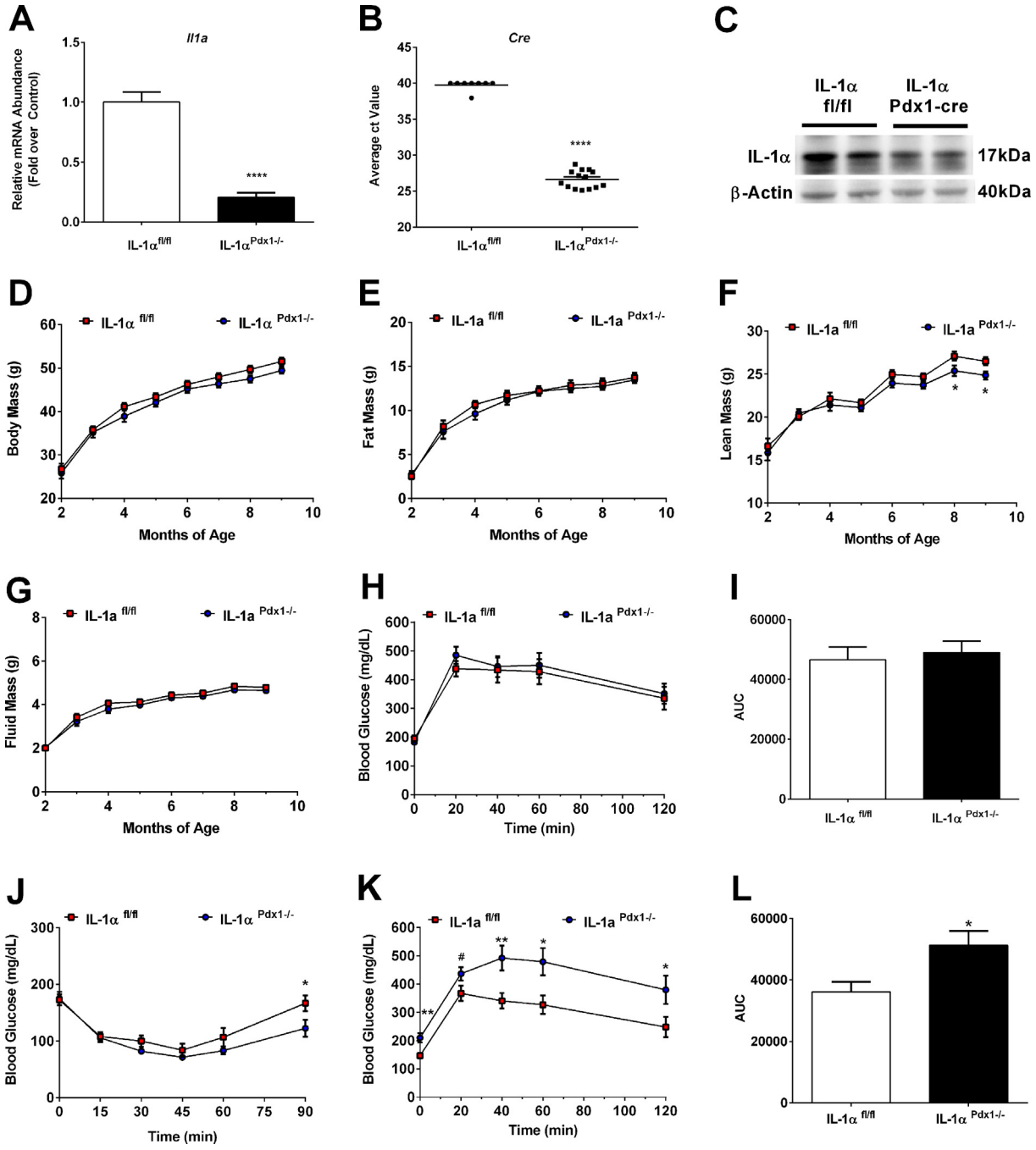

Figure 2: Deletion of IL-1α in pancreatic tissue impairs whole body glucose tolerance as male mice age. (A) *Il1a* and (B) *cre* expression in islets isolated from IL-1$\alpha^{fl/fl}$ and IL-1$\alpha^{Pdx1-/-}$ mice (n = 8–14 per group). (C) IL-1α abundance was determined in islets isolated from IL-1$\alpha^{fl/fl}$ and IL-1$\alpha^{Pdx1-/-}$ mice that were exposed to 10 ng/mL recombinant IL-1β for 4 h (n = 3 per group pooled and run in duplicate). (D) Body mass, (E) fat mass, (F) lean mass, and (G) fluid mass in male IL-1$\alpha^{fl/fl}$ and IL-1$\alpha^{Pdx1-/-}$ mice from 2 to 9 months of age. (H) GTT performed in 4-month-old male mice. (I) Area under the curve (AUC) for GTT shown in panel H. (J) ITT conducted in 2 month old male mice. (K) GTT performed in 8 month old male mice. (L) Area under the curve (AUC) for GTT shown in panel K. (A–B) n = 8–14 per group; (D–L) n = 9–16 per group. ****, $p < 0.0001$; **, $p < 0.01$; *, $p < 0.05$; #, $p < 0.10$.

decreased, circulating concentrations of insulin in the basal (unchallenged) condition were unchanged between groups (Figure 5D). However, we observed an overall reduction in pancreatic mass (data not shown), insulin-positive area (Figure 5E), and β-cell mass (Figure 5F) in male IL-1$\alpha^{Pdx1\ -/-}$ mice relative to controls. Measurements of the major and minor axis (conceptually depicted in Figure 5G) reveal reductions in both these parameters in IL-1$\alpha^{Pdx1-/-}$ mice compared to littermate controls (Figure 5H,I). Despite these changes, we found that the expression levels of *Aldh1a3* (de-differentiation) and *Sgk1* (growth) were unchanged (Supplementary Figs. 2E and 2F).

3.6. Generation of mice with a myeloid cell-specific deletion of IL-1α

Il1a expression is induced 5,702-fold in Raw 264.7 macrophages exposed to the pro-inflammatory stimulus LPS (Figure 6A), indicating robust production of this cytokine in response to a classic activation

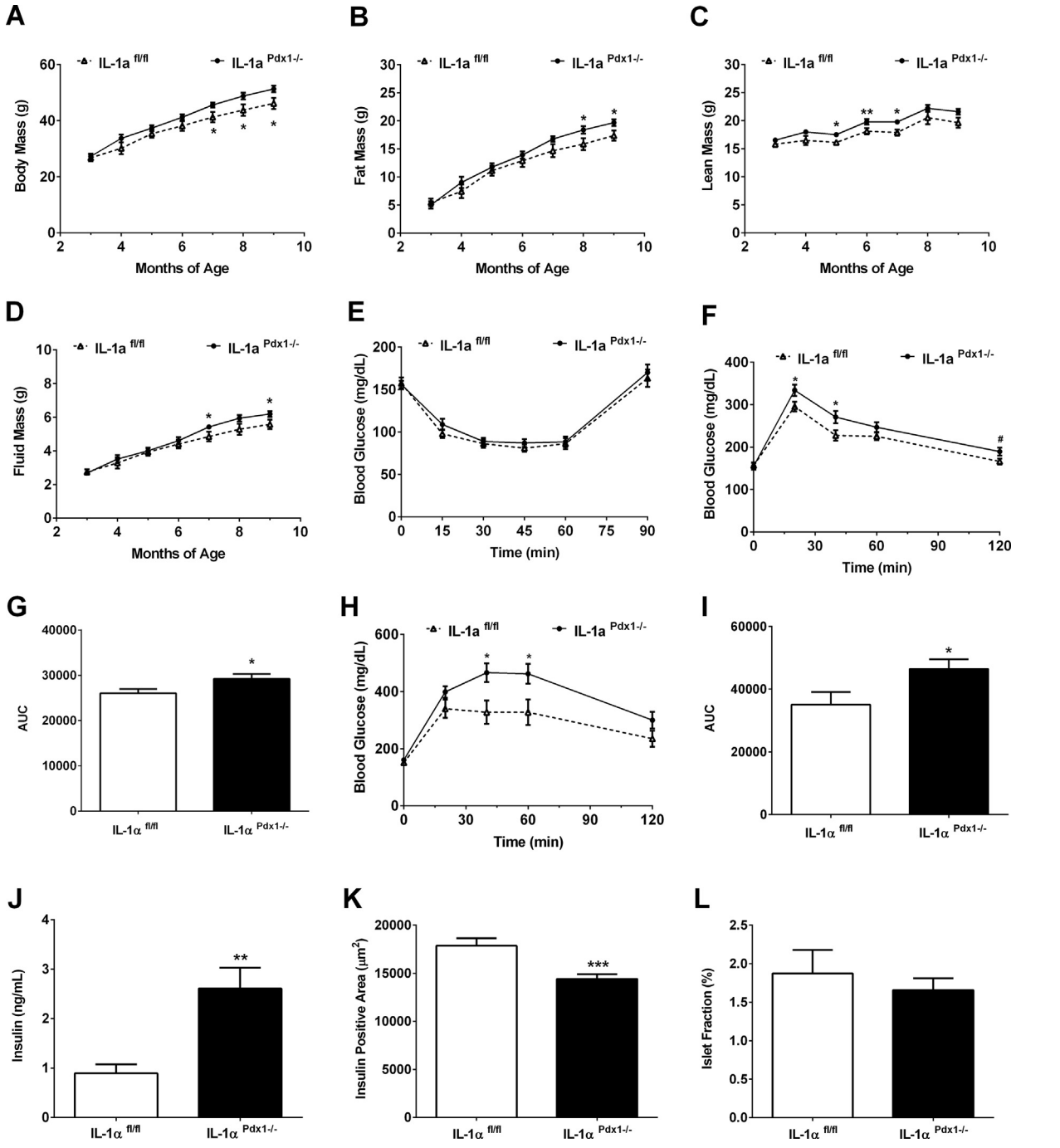

Figure 3: Pancreatic deletion of IL-1α negatively impacts body composition and reduces whole body glucose tolerance in female mice. (A) Body mass, (B) fat mass, (C) lean mass, and (D) fluid mass in female IL-1$\alpha^{fl/fl}$ and IL-1$\alpha^{Pdx1-/-}$ mice from 3 to 9 months of age. (E) ITT performed in 6-month-old female IL-1$\alpha^{fl/fl}$ and IL-1$\alpha^{Pdx1-/-}$ mice. (F—I) GTTs conducted in (F) 4 month and (H) 8-month-old female IL-1$\alpha^{fl/fl}$ and IL-1$\alpha^{Pdx1-/-}$ mice. (G) Area under the curve (AUC) for GTT shown in panel F. (I) Area under the curve (AUC) for GTT shown in panel H. (J) Serum insulin, (K) insulin positive area, and (L) islet fraction from 9-month-old female IL-1$\alpha^{fl/fl}$ and IL-1$\alpha^{Pdx1-/-}$ mice. n = 10—14 per group. ***, $p < 0.001$; **, $p < 0.01$; *, $p < 0.05$.

signal. As islet resident macrophages constantly display markers of the activated state [33], we next generated a myeloid-specific deletion, which includes macrophages, by breeding the IL-1$\alpha^{fl/fl}$ mice with mice expressing *cre* recombinase driven by the LysM promoter (IL-1$\alpha^{LysM-/-}$). In this novel cohort of mice, we examined IL-1α content in bone-marrow-derived macrophages stimulated with LPS. We found that IL-1α protein levels decreased by 62% in IL-1$\alpha^{LysM-/-}$ mice relative to littermate control mice (Figure 6B). Additionally, expression of the *Il1a* mRNA was reduced by 64% and 65%, respectively, in bone marrow-derived macrophages and peritoneal exudate cells of IL-1$\alpha^{LysM-/-}$ mice compared to control animals (Figure 6C). This reduction in expression of the *Il1a* gene is consistent with strong expression of the

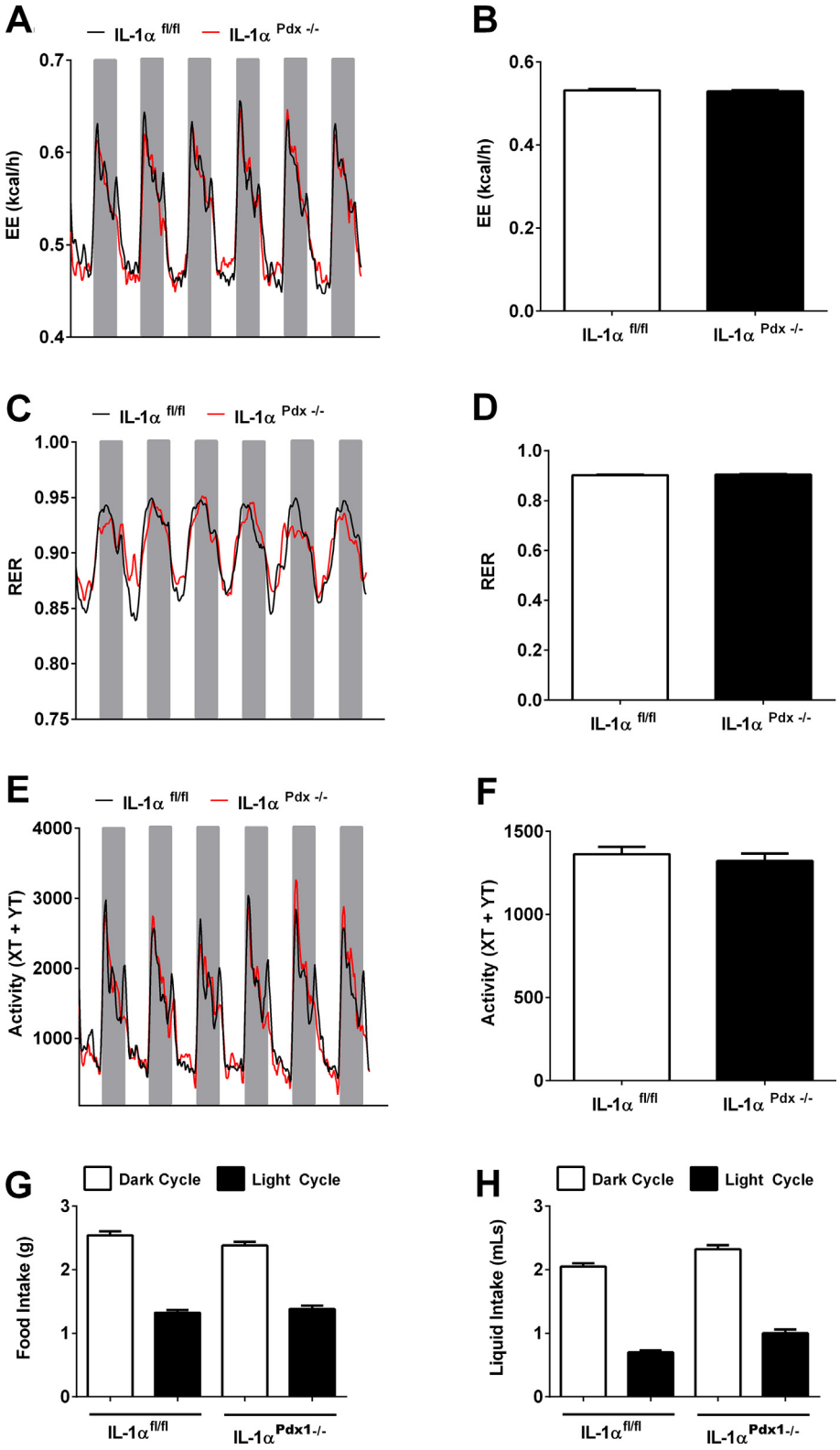

Figure 4: Pancreatic deletion of IL-1α does not modify energy expenditure (EE), respiratory exchange ratio (RER), physical activity, or food intake. (A) EE at daily intervals showing light cycle (white) or dark cycle (grey), and (B) mean EE over a 6-d period. (C) Respiratory exchange rate (RER) at daily intervals, and (D) mean RER over a 6-d period. (E) Activity, as measured by the number of X and Y beam breaks segregated by light (white) and dark cycle (grey shading), and (F) total activity over a 6-d period. (G) Total food (g) and (H) total liquid consumed (g) in male IL-1$\alpha^{fl/fl}$ and IL-1$\alpha^{Pdx1-/-}$ mice given by light (black bars) and dark cycle (white bars). n = 8 per group.

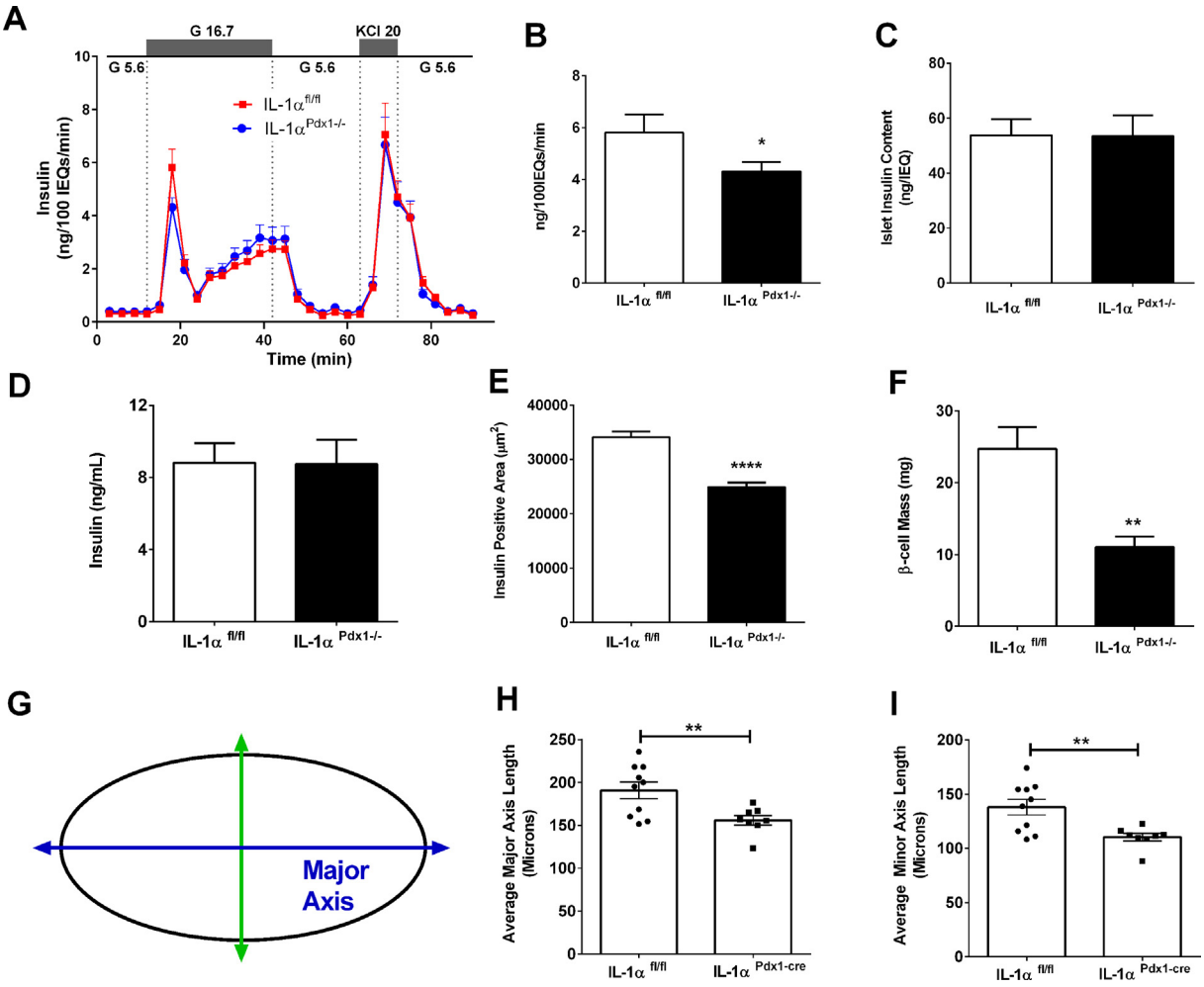

Figure 5: IL-1$\alpha^{Pdx1-/-}$ mice display a reduction in first phase glucose-stimulated insulin secretion and decreased islet β-cell mass. (A) Perifusion analysis from islets isolated from 4-month-old male IL-1$\alpha^{fl/fl}$ and IL-1$\alpha^{Pdx1-/-}$ mice. (B) Peak glucose-stimulated insulin output from the graph in A. (C) Insulin content per size-matched islets. (D) Serum insulin, (E) insulin positive area, (F) β-cell mass [calculated as (insulin positive area/total pancreas area) x pancreas wet weight]. Measurements of the major and minor axis (Figure 5G,H, I) from 9-month-old male IL-1$\alpha^{fl/fl}$ and IL-1$\alpha^{Pdx1-/-}$ mice. (A–C) n = 8 per group; (D) n = 30 per group; (E–I) n = 8–9 per group. ****, $p < 0.0001$; **, $p < 0.01$; *, $p < 0.05$.

cre transgene in each of these leukocyte populations (Figure 6D). Of note, the expression of the *Il1b* gene is unchanged in IL-1$\alpha^{LysM-/-}$ mice compared to IL-1$\alpha^{fl/fl}$ controls in both bone marrow-derived macrophages (Figure 6C) and peritoneal exudate cells (Figure 6C).

We also evaluated how IL-1α-deficient myeloid cells respond to an inflammatory stimulus using intraperitoneal injection of thioglycollate. Four days following exposure, peritoneal exudate was collected, and immune cell infiltrates were analyzed via flow cytometry. This experiment demonstrates that myeloid cell-specific deletion of IL-1α did not impair thioglycollate-induced macrophage recruitment (Figure 6E).

3.7. Myeloid cell-specific deletion of IL-1α does not alter body composition, glucose tolerance, or pancreatic β-cell mass in male or female mice

Both male and female IL-1$\alpha^{LysM-/-}$ and littermate control mice were fed a 25% fat (kcal) diet for 9 months. Over the course of time, both control and IL-1$\alpha^{LysM-/-}$ male mice showed similar age-related increases in body mass (Figure 7A), fat mass (Figure 7B), lean mass (Figure 7C), and fluid mass (Figure 7D). Similarly, no significant difference in total body mass or body composition was detected in female IL-1$\alpha^{LysM-/-}$ mice compared to IL-1$\alpha^{fl/fl}$ controls between 2 and 8 months of age (Suppl. Figs. 3A-C). Both young (12 weeks of age; Figure 7E) and older (7 months of age; Figure 7F) male mice exhibited similar responses to an insulin tolerance test. Furthermore, glucose tolerance remained similar between male IL-1$\alpha^{fl/fl}$ and IL-1$\alpha^{LysM-/-}$ mice at 4 months (Figures 7G and 8 months of age (Fig. 7H). Moreover, neither insulin sensitivity (Suppl. Figs. 3D-F) nor glucose tolerance (Suppl. Figs. 3G-I) are altered in young (16 weeks) or old (8 months) female IL-1$\alpha^{LysM-/-}$ mice compared to littermate controls. Serum insulin (Figure 7I), insulin positive area (Figure 7J), islet fraction (Figure 7K), and pancreas mass (Figure 7L) were similar between groups of male mice. In female mice, serum insulin concentrations are comparable between IL-1$\alpha^{fl/fl}$ and IL-1$\alpha^{LysM-/-}$ mice (Suppl. Fig. 3J). We note a significant decrease in insulin positive area in IL-1$\alpha^{LysM-/-}$ female mice compared to controls (Suppl. Fig. 3K), although islet fraction is unchanged between groups (Suppl. Fig. 3L).

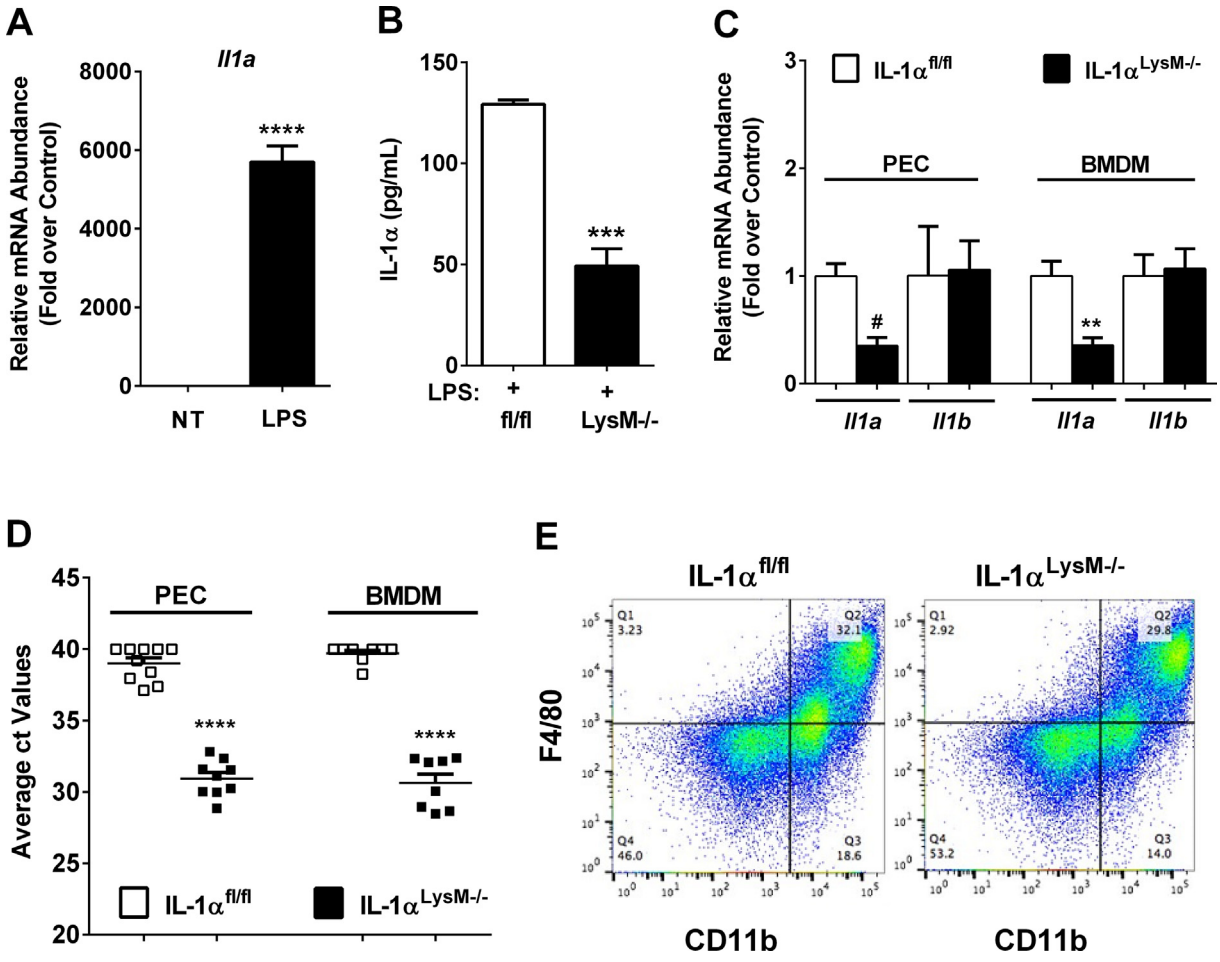

Figure 6: Generation of mice with a myeloid cell-specific deletion of IL-1α. (A) qPCR analysis of *Il1a* transcript levels from Raw 264.7 cells untreated or treated with 1 μg/mL LPS for 6 h. (B) IL-1α protein content in LPS-stimulated BMDMs from male IL-1$\alpha^{fl/fl}$ and IL-1$\alpha^{LysM-/-}$ mice (n = 2 in duplicate per group). (C) *Il1a* and *Il1b* expression in LPS-stimulated BMDMs and PECs. (D) *cre* expression in BMDMs and PECs harvested from IL-1$\alpha^{fl/fl}$ and IL-1$\alpha^{LysM-/-}$ mice (n = 9–13 per group). (E) PECs from IL-1$\alpha^{fl/fl}$ and IL-1$\alpha^{LysM-/-}$ mice were stimulated with LPS and stained with antibodies against CD11b and F4/80. ****, $p < 0.0001$ vs. NT; #, $p < 0.0001$ vs. respective IL-1$\alpha^{fl/fl}$ control; ***, $p < 0.001$ vs. respective IL-1$\alpha^{fl/fl}$ control; **p < 0.01 vs. respective littermate control; *, $p < 0.05$ vs. respective IL-1$\alpha^{fl/fl}$ control.

3.8. Myeloid-specific deletion of IL-1α does not alter respiratory quotient (RQ), energy expenditure, activity, or caloric intake in male mice

With no changes in glucose tolerance or insulin sensitivity detected in IL-1$\alpha^{LysM-/-}$ mice, we investigated whether myeloid-specific IL-1α might regulate respiratory quotient, energy expenditure, activity, or caloric intake. Over a 7-d period, no detectable change in RQ was seen between groups of mice either during the light or dark cycle (Figure 8A,B). Similarly, energy expenditure was equivalent between groups across a 7 d period (Figure 8C,D). Furthermore, deletion of IL-1α in myeloid cells did not impact food intake (Figure 8E), liquid consumption (Figure 8F), or total activity (not shown).

4. DISCUSSION

Cytokines of the interleukin-1 family are largely known for their roles in inflammation and inflammation-related outcomes. Studies investigating IL-1R signaling in islet β-cells have largely been conducted using cell lines or islets exposed to cytokines in culture, offering interesting insights into signaling pathways and the deleterious consequences of prolonged IL-1R activation *in vitro* [34–36]. However, the tissue-specific contributions of IL-1R and its associated ligands to glucose homeostasis *in vivo* has only recently been addressed [25,37]. For elucidating these important *in vivo* biological responses, we generated mice with a conditional allele for *Il1a*. Using this novel tissue-targeted *in vivo* model, we investigated the contribution of IL-1α from cells of the myeloid lineage versus pancreatic tissue.

Our approach is significant because tissue resident macrophages produce a variety of cytokines required for islet development as well as influence islet function in adult mammalian species [38–40]. Along these lines, we found that the gene encoding IL-1α was highly inducible in mouse, rat, and human islets as well as in cultured rat-derived β-cell lines (Figure 1C–G). In addition, macrophages express IL-1α in the basal state as well as enhance its expression upon exposure to an inflammatory stimulus (Figure 6A and data not shown). However, IL-1α deletion from cells of the myeloid lineage, which includes macrophages and monocytes, had no effect on whole body glucose homeostasis (Figure 7G–H) or islet β-cell morphology (Figure 7J–L). This finding was interesting considering that recombinant IL-1α added to isolated cultured islets increases insulin output acutely [14]. We observed a modest but significant reduction in insulin-

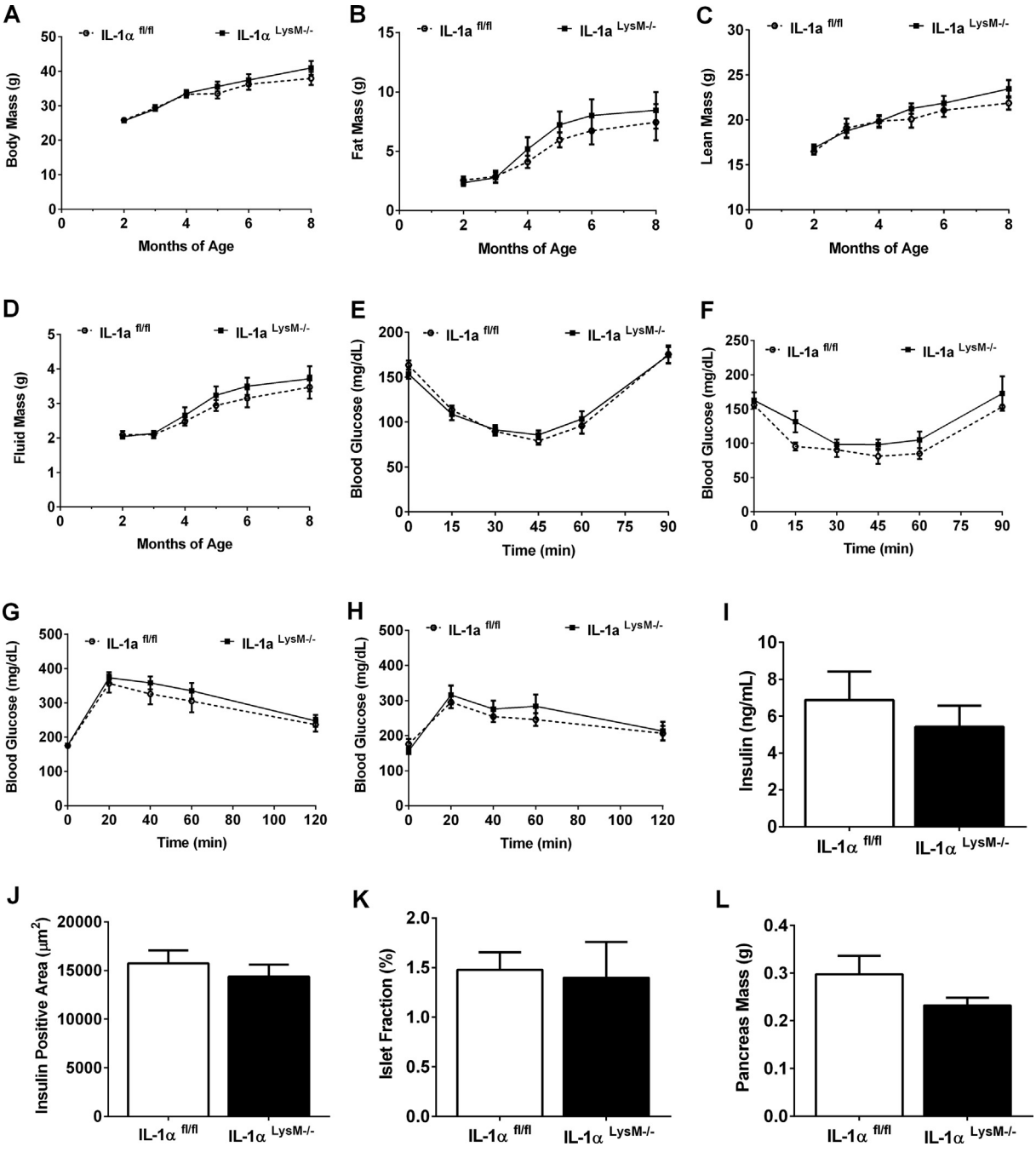

Figure 7: Myeloid cell-specific deletion of IL-1α does not alter body composition, glucose tolerance, or pancreatic β-cell mass in male mice. (A) Body mass, (B) fat mass, (C) lean mass, and (D) fluid mass in male IL-1$\alpha^{fl/fl}$ and IL-1$\alpha^{LysM-/-}$ mice from 2 to 8 months of age. Insulin tolerance tests (ITT) performed in (E) 3-month and (F) 7-month-old male IL-1$\alpha^{fl/fl}$ and IL-1$\alpha^{LysM-/-}$ mice. Glucose tolerance tests (GTT) conducted in (G) 4 month and (H) 8-month-old male IL-1$\alpha^{fl/fl}$ and IL-1$\alpha^{LysM-/-}$ mice. (I) Serum insulin, (J) insulin positive area, (K) islet fraction, and (L) pancreas mass from 9-month-old male IL-1$\alpha^{fl/fl}$ and IL-1$\alpha^{LysM-/-}$ mice. n = 11–14 per group.

positive area in female IL-1$\alpha^{LysM-/-}$ mice (Supp. Fig. 1K) that is not seen in male IL-1$\alpha^{LysM-/-}$ mice (Figure 7J).

Coupled with our findings that IL-1α expression is markedly elevated in pancreatic islets isolated from rodent models of obesity and pure populations of cultured β-cell lines exposed to IL-1β, we also conducted studies using pancreatic-targeted deletion of IL-1α; this includes loss of IL-1α from pancreatic β-cells *in vivo* [41]. These experiments revealed that IL-1α within pancreatic tissue is critical for maintaining glucose homeostasis during the ageing process in both male and female mice (Figures 2 and 3). The observed phenotype was not due to changes in energy expenditure, respiratory quotient, physical activity, or caloric intake (Figure 4). Instead, we found that glucose-stimulated insulin secretion was reduced in IL-1$\alpha^{Pdx1-/-}$ mice compared to littermate controls (Figure 5A,B; Suppl. Fig. 2B) without significant changes in islet insulin content (Figure 5C; Suppl. Fig. 2A) or peripheral insulin sensitivity (Figures 2J and 3E). We found a significant difference at the 90-min time point of the insulin tolerance test in male mice, which may indicate a difference in

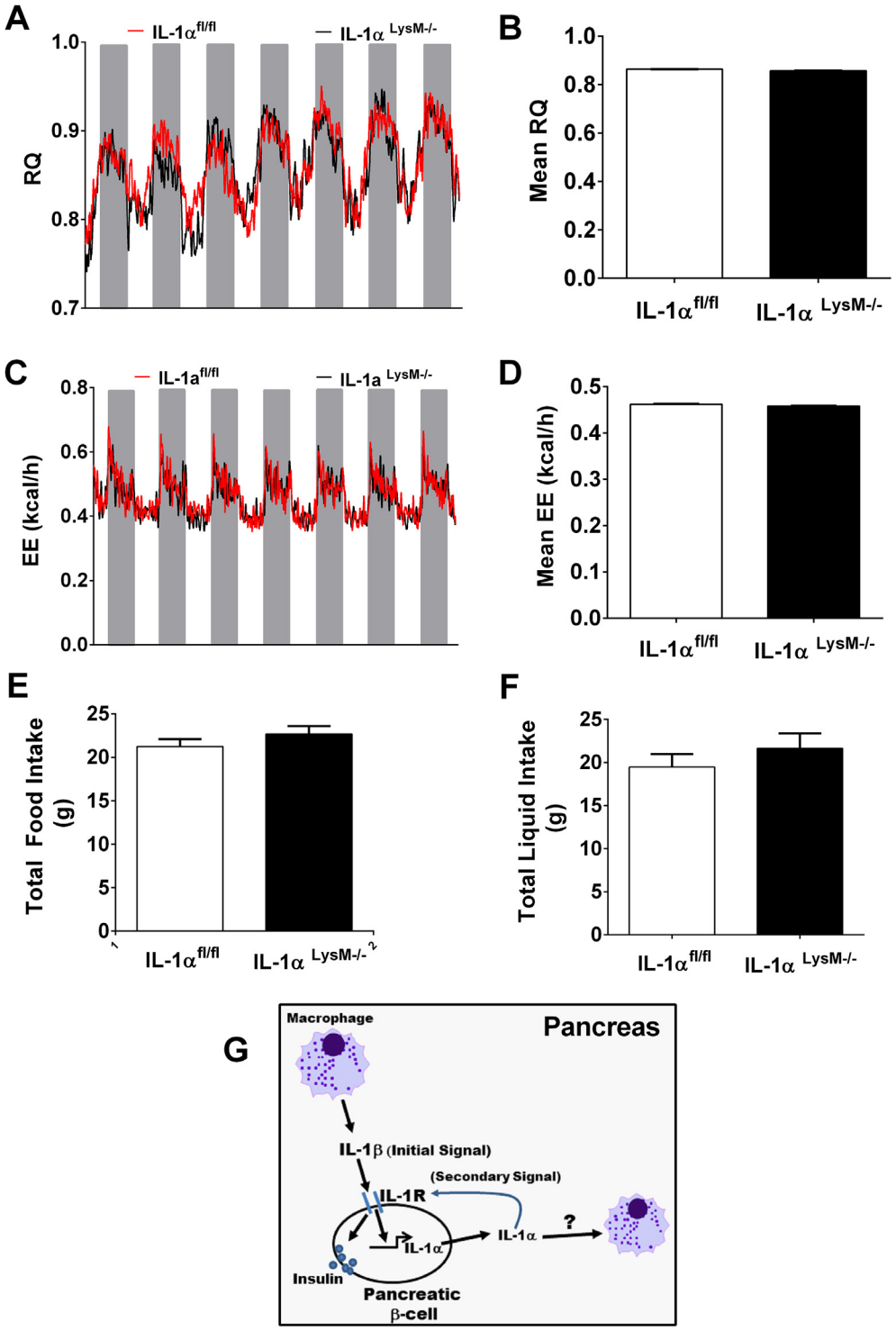

Figure 8: Myeloid-specific deletion of IL-1α does not alter respiratory quotient, energy expenditure, activity, sleep time, or caloric intake. (A) Respiratory quotient (RQ) at daily intervals showing light cycle (white) or dark cycle (grey). (B) Mean RQ across all time points over a 7-d period. (C) Energy expenditure (EE) at daily intervals and (D) mean EE. (E) Total food consumed in a 7-d period (g) and (F) total liquid consumed in a 7-d period (g). n = 8 per group. (G) Schematic illustrating that IL-1R activation by IL-1β (initial signal) drives the production of IL-1α. IL-1α (secondary signal) supports both insulin secretion and growth of endocrine and exocrine tissue (not pictured), while conceivably also influencing the status of tissue resident immune cells. The question mark indicates that a specific type of action (e.g., change in gene expression, chemotaxis, etc.) on tissue resident immune cells is not established at present.

counter-regulatory responses between genotypes, while insulin-mediated glucose disposal (15—60 min) was not different between the groups (Figure 2J). In addition, there was reduced total pancreatic mass (not shown), decreased insulin positive cell mass (Figure 5E), and less total islet β-cell mass in the IL-1α$^{Pdx1-/-}$ mice (Figure 5F). In looking at the major and minor axis lengths of >1,500 islets per genotype, we found that both the major and minor axis was reduced in the IL-1α$^{Pdx1-/-}$ mice (Figure 5G-I).

We interpret these data to indicate that the IL-1α from pancreatic tissue has an important role to support glucose homeostasis and islet size by regulating glucose-stimulated insulin secretion, total pancreatic mass, and islet β-cell mass. In support of this idea, IL-1α gene expression is elevated in rat (Figure 1A) and mouse (Figure 1B) models of obesity, which we interpret as a compensatory autocrine/paracrine response to enhance β-cell growth and function during periods of increased workload. Additional support for this idea comes from pancreatic-targeted deletion of the IL-1R [25] and myeloid-specific deletion of IL-1β [24], which both show reductions in insulin secretion capabilities. Collectively, these studies expand our understanding of the important physiologic relationship that exists between islet resident macrophages (secreting IL-1β) and β-cells producing IL-1α as well as responding to both IL-1α and IL-1β via the IL-1R. There are several possible ways IL-1α could be supporting islet β-cell function or contributing to growth. The first is by fine tuning responses through the IL-1R in conjunction with IL-1β secreted by tissue resident macrophages. The second is through altering transcriptional patterns inside the cell (non-secreted function) [42]. The third is by having a separate effect from that of IL-1β when activating the IL-1R, a concept known as 'selective bias' or 'biased agonism" for other cell-surface receptors [43]. A final important consideration is that the *in vivo* deletion used here was likely present throughout the life span; it is thus possible that an inducible deletion in the adult mouse will provide important complementary information.

Reductions in islet β-cell mass and/or inherited deficiencies in islet β—cell function compromise glucose tolerance and increase risk of diabetes [44—46]. Overall, this concept has been modeled experimentally by loss of function studies targeting a variety of key islet β-cell enriched transcription factors [47—50]. Our novel data show for the first time that the cytokine IL-1α is a critical growth factor and possible potent autocrine/paracrine signaling contributor supporting islet β-cell insulin secretion as well as assisting with growth of pancreatic endocrine and exocrine tissue (Figure 8G). Whether IL-1α derived from pancreatic tissue also influences the tissue resident macrophage population (either as a chemoattractant, stimulation signal, or growth factor) is unclear at present, but warrants further consideration. Collectively, these findings have important translational implications considering the array of therapies designed to target the IL-1R pathway, including the individual cytokine ligands.

Indeed, several clinical approaches that either target the IL-1R directly, or alternatively, inhibit the activity of IL-1α or IL-1β have been developed. For example, anakinra is a recombinant version of the human IL-1R antagonist, which was established based on the biology of the endogenously produced protein [51—53]. Early uses of anakinra were for systemic inflammatory diseases, such as rheumatoid arthritis [54]. Later uses targeted patients with Type 2 diabetes, where lowering of glycated hemoglobin and C-reactive peptide (systemic inflammation marker) were observed [55]. However, the clinical use of anakinra was not effective in patients with Type 1 diabetes [56]. It is difficult to untangle the important physiological effects of IL-1R activation from the pathophysiological outcomes associated with overactive IL-1R signaling using the aforementioned systemic approaches. This view is supported by tissue-specific deletions of IL-1R [25] and interleukin-1β [24], where myeloid-derived IL-1β and pancreas IL-1R were critical for maintenance of insulin output and overall glucose homeostasis *in vivo*.

In addition, we now show that IL-1R activation by IL-1β induces the IL-1α gene in pancreatic β-cells (Figure 1C—G), suggesting a cytokine 'circuit' that promotes overall β-cell health (Figure 8G). Thus, studies identifying tissue-specific actions of signals traditionally associated with inflammation (such as cytokines) are critical to separate their physiological roles from their pathophysiological outcomes. We note that the detrimental outcomes associated with IL-1α or IL-1β are likely to be due to overstimulation of the IL-1R, producing non-resolving inflammation in response to these cytokines. This is in contrast to their regulated activity, which is clearly required for proper tissue health and function.

In summary, we describe a conditional deletion of IL-1α using myeloid- and pancreatic-specific approaches and document the important role of pancreatic-derived IL-1α to support insulin secretion, β-cell mass, and glucose homeostasis *in vivo*. Our results using these novel mouse lines reveal that the cytokine IL-1α is an important regulatory determinant for growth of pancreatic islet tissue as well as for supporting physiological glucose-stimulated insulin secretion.

FUNDING SOURCES

This study used PBRC core facilities (Genomics, Cell Biology and Bioimaging, and Transgenics) that are supported in part by COBRE (P20 RR021945 and P30 GM118430) and NORC (P30 DK072476) center grants from the National Institutes of Health, as well as equipment purchased with funds from a shared instrumentation grant (NIH S10 OD023703). These studies were also supported in part by National Institutes of Health grants R21 AI138136 (JJC), R01 DK123183 (JJC), U54 GM104940 (SJB), and P20 GM135002 (SJB). Finally, we acknowledge the use of the Islet Procurement and Analysis Core of the Vanderbilt Diabetes Research and Training Center supported by NIH grant P30 DK020593.

ACKNOWLEDGMENTS

The authors thank colleagues at PBRC for their support and critical evaluation of this work.

CONFLICT OF INTEREST

The authors declare that they have no conflicts of interest with the contents of this article.

APPENDIX A. SUPPLEMENTARY DATA

Supplementary data to this article can be found online at https://doi.org/10.1016/j.molmet.2020.101140.

REFERENCES

[1] Dinarello, C.A., Goldin, N.P., Wolff, S.M., 1974. Demonstration and characterization of two distinct human leukocytic pyrogens. Journal of Experimental Medicine 139(6):1369—1381.

[2] March, C.J., Mosley, B., Larsen, A., Cerretti, D.P., Braedt, G., Price, V., et al., 1985. Cloning, sequence and expression of two distinct human interleukin-1 complementary DNAs. Nature 315(6021):641—647.

[3] O'Neill, L.A., 1996. Interleukin I receptors and signal transduction. Biochemical Society Transactions 24(1):207—211.

[4] Sims, J.E., Gayle, M.A., Slack, J.L., Alderson, M.R., Bird, T.A., Giri, J.G., et al., 1993. Interleukin 1 signaling occurs exclusively via the type I receptor. Proceedings of the National Academy of Sciences of the U S A 90(13):6155–6159.

[5] Burke, S.J., Collier, J.J., 2015. Transcriptional regulation of chemokine genes: a link to pancreatic islet inflammation? Biomolecules 5(2):1020–1034.

[6] Collier, J.J., Sparer, T.E., Karlstad, M.D., Burke, S.J., 2017. Pancreatic islet inflammation: an emerging role for chemokines. Journal of Molecular Endocrinology 59(1):R33–R46.

[7] O'Neill, L.A., Greene, C., 1998. Signal transduction pathways activated by the IL-1 receptor family: ancient signaling machinery in mammals, insects, and plants. Journal of Leukocyte Biology 63(6):650–657.

[8] Gahring, L.C., Buckley, A., Daynes, R.A., 1985. Presence of epidermal-derived thymocyte activating factor/interleukin 1 in normal human stratum corneum. Journal of Clinical Investigation 76(4):1585–1591.

[9] Hauser, C., Saurat, J.H., Schmitt, A., Jaunin, F., Dayer, J.M., 1986. Interleukin 1 is present in normal human epidermis. The Journal of Immunology 136(9):3317–3323.

[10] Nathan, C.F., 1987. Secretory products of macrophages. Journal of Clinical Investigation 79(2):319–326.

[11] Marsh, C.B., Lowe, M.P., Rovin, B.H., Parker, J.M., Liao, Z., Knoell, D.L., et al., 1998. Lymphocytes produce IL-1beta in response to Fcgamma receptor cross-linking: effects on parenchymal cell IL-8 release. The Journal of Immunology 160(8):3942–3948.

[12] Kobayashi, Y., Yamamoto, K., Saido, T., Kawasaki, H., Oppenheim, J.J., Matsushima, K., 1990. Identification of calcium-activated neutral protease as a processing enzyme of human interleukin 1 alpha. Proceedings of the National Academy of Sciences of the U S A 87(14):5548–5552.

[13] Martinon, F., Burns, K., Tschopp, J., 2002. The inflammasome: a molecular platform triggering activation of inflammatory caspases and processing of proIL-beta. Molecular Cell 10(2):417–426.

[14] Zawalich, W.S., Zawalich, K.C., Rasmussen, H., 1989. Interleukin-1 alpha exerts glucose-dependent stimulatory and inhibitory effects on islet cell phosphoinositide hydrolysis and insulin secretion. Endocrinology 124(5):2350–2357.

[15] Zawalich, W.S., Zawalich, K.C., 1989. Interleukin 1 is a potent stimulator of islet insulin secretion and phosphoinositide hydrolysis. American Journal of Physiology 256(1 Pt 1):E19–E24.

[16] Burke, S.J., Stadler, K., Lu, D., Gleason, E., Han, A., Donohoe, D.R., et al., 2015. IL-1beta reciprocally regulates chemokine and insulin secretion in pancreatic beta-cells via NF-kappaB. American Journal of Physiology. Endocrinology and Metabolism 309(8):E715–E726.

[17] Burke, S.J., Lu, D., Sparer, T.E., Masi, T., Goff, M.R., Karlstad, M.D., et al., 2014. NF-kappaB and STAT1 control CXCL1 and CXCL2 gene transcription. American Journal of Physiology. Endocrinology and Metabolism 306(2):E131–E149.

[18] Burke, S.J., Collier, J.J., 2011. The gene encoding cyclooxygenase-2 is regulated by IL-1beta and prostaglandins in 832/13 rat insulinoma cells. Cellular Immunology 271(2):379–384.

[19] Southern, C., Schulster, D., Green, I.C., 1990. Inhibition of insulin secretion by interleukin-1 beta and tumour necrosis factor-alpha via an L-arginine-dependent nitric oxide generating mechanism. FEBS Letters 276(1–2):42–44.

[20] Boni-Schnetzler, M., Boller, S., Debray, S., Bouzakri, K., Meier, D.T., Prazak, R., et al., 2009. Free fatty acids induce a proinflammatory response in islets via the abundantly expressed interleukin-1 receptor I. Endocrinology 150(12):5218–5229.

[21] Scarim, A.L., Arnush, M., Hill, J.R., Marshall, C.A., Baldwin, A., McDaniel, M.L., et al., 1997. Evidence for the presence of type I IL-1 receptors on beta-cells of islets of Langerhans. Biochimica et Biophysica Acta 1361(3):313–320.

[22] Hajmrle, C., Smith, N., Spigelman, A.F., Dai, X., Senior, L., Bautista, A., et al., 2016. Interleukin-1 signaling contributes to acute islet compensation. JCI Insight 1(4):e86055.

[23] Scarim, A.L., Heitmeier, M.R., Corbett, J.A., 1997. Irreversible inhibition of metabolic function and islet destruction after a 36-hour exposure to interleukin-1beta. Endocrinology 138(12):5301–5307.

[24] Dror, E., Dalmas, E., Meier, D.T., Wueest, S., Thevenet, J., Thienel, C., et al., 2017. Postprandial macrophage-derived IL-1beta stimulates insulin, and both synergistically promote glucose disposal and inflammation. Nature Immunology 18(3):283–292.

[25] Burke, S.J., Batdorf, H.M., Burk, D.H., Martin, T.M., Mendoza, T., Stadler, K., et al., 2018. Pancreatic deletion of the interleukin-1 receptor disrupts whole body glucose homeostasis and promotes islet beta-cell de-differentiation. Mol Metab 14:95–107.

[26] Hohmeier, H.E., Mulder, H., Chen, G., Henkel-Rieger, R., Prentki, M., Newgard, C.B., 2000. Isolation of INS-1-derived cell lines with robust ATP-sensitive K+ channel-dependent and -independent glucose-stimulated insulin secretion. Diabetes 49(3):424–430.

[27] Burke, S.J., Karlstad, M.D., Regal, K.M., Sparer, T.E., Lu, D., Elks, C.M., et al., 2015. CCL20 is elevated during obesity and differentially regulated by NF-kappaB subunits in pancreatic beta-cells. Biochimica et Biophysica Acta 1849(6):637–652.

[28] Burke, S.J., Batdorf, H.M., Martin, T.M., Burk, D.H., Noland, R.C., Cooley, C.R., et al., 2018. Liquid sucrose consumption promotes obesity and impairs glucose tolerance without altering circulating insulin levels. Obesity 26(7):1188–1196.

[29] Burke, S.J., Batdorf, H.M., Eder, A.E., Karlstad, M.D., Burk, D.H., Noland, R.C., et al., 2017. Oral corticosterone administration reduces insulitis but promotes insulin resistance and hyperglycemia in male nonobese diabetic mice. American Journal Of Pathology 187(3):614–626.

[30] Wang, T., Lacik, I., Brissova, M., Anilkumar, A.V., Prokop, A., Hunkeler, D., et al., 1997. An encapsulation system for the immunoisolation of pancreatic islets. Nature Biotechnology 15(4):358–362.

[31] Burke, S.J., Batdorf, H.M., Burk, D.H., Noland, R.C., Eder, A.E., Boulos, M.S., et al., 2017. Db/db mice exhibit features of human type 2 diabetes that are not present in weight-matched C57BL/6J mice fed a western diet. Journal of diabetes research 2017:8503754.

[32] Hasnain, S.Z., Borg, D.J., Harcourt, B.E., Tong, H., Sheng, Y.H., Ng, C.P., et al., 2014. Glycemic control in diabetes is restored by therapeutic manipulation of cytokines that regulate beta cell stress. Nature Medicine 20(12):1417–1426.

[33] Ferris, S.T., Zakharov, P.N., Wan, X., Calderon, B., Artyomov, M.N., Unanue, E.R., et al., 2017. The islet-resident macrophage is in an inflammatory state and senses microbial products in blood. Journal of Experimental Medicine 214(8):2369–2385.

[34] Corbett, J.A., Wang, J.L., Sweetland, M.A., Lancaster Jr., J.R., McDaniel, M.L., 1992. Interleukin 1 beta induces the formation of nitric oxide by beta-cells purified from rodent islets of Langerhans. Evidence for the beta-cell as a source and site of action of nitric oxide. Journal of Clinical Investigation 90(6):2384–2391.

[35] Tran, V.V., Chen, G., Newgard, C.B., Hohmeier, H.E., 2003. Discrete and complementary mechanisms of protection of beta-cells against cytokine-induced and oxidative damage achieved by bcl-2 overexpression and a cytokine selection strategy. Diabetes 52(6):1423–1432.

[36] Burke, S.J., Goff, M.R., Lu, D., Proud, D., Karlstad, M.D., Collier, J.J., 2013. Synergistic expression of the CXCL10 gene in response to IL-1beta and IFN-gamma involves NF-kappaB, phosphorylation of STAT1 at Tyr701, and acetylation of histones H3 and H4. The Journal of Immunology 191(1):323–336.

[37] Boni-Schnetzler, M., Hauselmann, S.P., Dalmas, E., Meier, D.T., Thienel, C., Traub, S., et al., 2018. Beta cell-specific deletion of the IL-1 receptor antagonist impairs beta cell proliferation and insulin secretion. Cell Reports 22(7):1774–1786.

[38] Dalmas, E., 2019. Innate immune priming of insulin secretion. Current Opinion in Immunology 56:44–49.

[39] Calderon, B., Carrero, J.A., Ferris, S.T., Sojka, D.K., Moore, L., Epelman, S., et al., 2015. The pancreas anatomy conditions the origin and properties of resident macrophages. Journal of Experimental Medicine 212(10):1497–1512.

[40] Banaei-Bouchareb, L., Gouon-Evans, V., Samara-Boustani, D., Castellotti, M.C., Czernichow, P., Pollard, J.W., et al., 2004. Insulin cell mass is altered in Csf1op/Csf1op macrophage-deficient mice. Journal of Leukocyte Biology 76(2):359–367.

[41] Magnuson, M.A., Osipovich, A.B., 2013. Pancreas-specific Cre driver lines and considerations for their prudent use. Cell Metabolism 18(1):9–20.

[42] Werman, A., Werman-Venkert, R., White, R., Lee, J.K., Werman, B., Krelin, Y., et al., 2004. The precursor form of IL-1alpha is an intracrine proinflammatory activator of transcription. Proceedings of the National Academy of Sciences of the U S A 101(8):2434–2439.

[43] Wisler, J.W., Xiao, K., Thomsen, A.R., Lefkowitz, R.J., 2014. Recent developments in biased agonism. Current Opinion in Cell Biology 27:18–24.

[44] Meier, J.J., Bonadonna, R.C., 2013. Role of reduced beta-cell mass versus impaired beta-cell function in the pathogenesis of type 2 diabetes. Diabetes Care 36(Suppl 2):S113–S119.

[45] Burke, S.J., Karlstad, M.D., Collier, J.J., 2016. Pancreatic islet responses to metabolic trauma. Shock 46(3):230–238.

[46] Weir, G.C., Gaglia, J., Bonner-Weir, S., 2020. Inadequate beta-cell mass is essential for the pathogenesis of type 2 diabetes. Lancet Diabetes Endocrinol 8(3):249–256.

[47] Guo, S., Dai, C., Guo, M., Taylor, B., Harmon, J.S., Sander, M., et al., 2013. Inactivation of specific beta cell transcription factors in type 2 diabetes. Journal of Clinical Investigation 123(8):3305–3316.

[48] Zhang, C., Moriguchi, T., Kajihara, M., Esaki, R., Harada, A., Shimohata, H., et al., 2005. MafA is a key regulator of glucose-stimulated insulin secretion. Molecular and Cellular Biology 25(12):4969–4976.

[49] Schisler, J.C., Jensen, P.B., Taylor, D.G., Becker, T.C., Knop, F.K., Takekawa, S., et al., 2005. The Nkx6.1 homeodomain transcription factor suppresses glucagon expression and regulates glucose-stimulated insulin secretion in islet beta cells. Proceedings of the National Academy of Sciences of the U S A 102(20):7297–7302.

[50] Gao, T., McKenna, B., Li, C., Reichert, M., Nguyen, J., Singh, T., et al., 2014. Pdx1 maintains beta cell identity and function by repressing an alpha cell program. Cell Metabolism 19(2):259–271.

[51] Malyak, M., Guthridge, J.M., Hance, K.R., Dower, S.K., Freed, J.H., Arend, W.P., 1998. Characterization of a low molecular weight isoform of IL-1 receptor antagonist. The Journal of Immunology 161(4):1997–2003.

[52] Arend, W.P., Malyak, M., Guthridge, C.J., Gabay, C., 1998. Interleukin-1 receptor antagonist: role in biology. Annual Review of Immunology 16:27–55.

[53] Arend, W.P., 1991. Interleukin 1 receptor antagonist. A new member of the interleukin 1 family. Journal of Clinical Investigation 88(5):1445–1451.

[54] Cohen, S.B., Rubbert, A., 2003. Bringing the clinical experience with anakinra to the patient. Rheumatology 42(Suppl 2):36–40.

[55] Larsen, C.M., Faulenbach, M., Vaag, A., Volund, A., Ehses, J.A., Seifert, B., et al., 2007. Interleukin-1-receptor antagonist in type 2 diabetes mellitus. New England Journal of Medicine 356(15):1517–1526.

[56] Moran, A., Bundy, B., Becker, D.J., DiMeglio, L.A., Gitelman, S.E., Goland, R., et al., 2013. Interleukin-1 antagonism in type 1 diabetes of recent onset: two multicentre, randomised, double-blind, placebo-controlled trials. Lancet 381(9881):1905–1915.

